

GEOLOGY FOR SOCIETY

SINCE 1858



**GEOLOGICAL
SURVEY OF
NORWAY**

· NGU ·



NGU REPORT
2022.030

Preliminary inventory of rock avalanche
deposits and their related sources in Norway.
Regional distribution, main features and
topographic constraints



Report no.: 2022.030	ISSN: 0800-3416 (print) ISSN: 2387-3515 (online)	Grading:	
Title: Preliminary inventory of rock avalanche deposits and their related sources in Norway. Regional distribution, main features and topographic constraints			
Authors: Penna, I.M., Nicolet, P., Hermanns, R.L., Böhme, M., Noël, F:		Client: NVE	
County: Norway		Commune: -	
Map-sheet name (M=1:250.000): -		Map-sheet no. & name (M1:50.000): -	
Deposit name and grid-reference: -		Number of pages: Price (NOK): Map enclosures: -	
Fieldwork carried out: -	Date of report: 05.12.2022	Project no.: 393400	Person responsible: Jacob Bendle
Summary <p>In this report we have assessed some of the characteristics of the 248 rock avalanche deposits (rock slope failure deposits and their related source areas) inventoried in Norway up to date. These pre-historic and historic rock avalanche deposits are mostly located in the North (Troms and Finnmark counties) and in the South (Vestland and Møre og Romsdal counties) of Norway. Their spatial distribution is clearly correlated to relief conditions. The lithologies involved in the rock avalanche events in the North and the South differ, which can be related to different dominant lithologies in both regions. The identified deposits are present on land, in fjords and lakes, or a combination of those. Some are very well preserved, while others have been eroded by rivers or buried by fluvial deposits. Our work shows that the mobility of the rock avalanches is correlated to the slope conditions. A preliminary result is that mobility on average decreases with increasing slope angle. This relation, that has not been documented in previous studies, could be related to energy loss under particular topographic conditions in deeply glacially eroded valleys. While we investigate a significant number of past rock avalanche events in this report, systematic mapping at the national scale is likely to (i) shed light on the uncertainties identified in this report, (ii) provide data with the potential to improve the understanding of rock avalanche occurrence and dynamics, and (iii) generate baseline data for improved assessment of run-out length of future rock avalanche scenarios.</p>			
Keywords			
Rock avalanche deposits	Mobility	Run-out length	
Lithological constraints	Significant relief	Volume assessment	

Table of contents

1. INTRODUCTION	5
2. Methodology	7
2.1 Mapping of rock avalanches - Inventory	7
2.2 Significant relief	7
2.3 Longitudinal profiles and cumulative curves	8
2.4 Computation of orientation and slope aspect of source areas	9
2.5 Computation of volumes involved in rock avalanches.....	9
2.6 Angle of reach and Statistical analysis	10
1. Results	10
2.7 Mapping of rock avalanches	10
2.8 Rock avalanche occurrence and significant relief	13
2.9 Rock avalanches and lithologies	14
2.10 Slope aspects and slope of source area	14
2.11 Volume estimates.....	15
2.12 Run-out and angles of reach of rock avalanches	18
3. Discussion and conclusions	22
3.1 Conditioning factors of rock avalanche occurrence and mobility	22
3.2 Completeness of the inventory	24
4. References	25

1. INTRODUCTION

Rock avalanches form by the collapse of a rock mass that disintegrates and propagates as a granular flow with high speed (Evans et al., 2006; Hungr et al., 2014; Hermanns et al., 2022). In this report, we use the term “rock avalanche” as the translation from the Norwegian term “fjellskred”. This term is defined as a large landslide sourcing preliminary from rock, in the order of hundred thousand to several million cubic meters, in which the rock mass moves down quickly along the slope (NVE rapport 14/2011). They have typical morphology of a flow component during the run out of the event. Following the Norwegian term, the lower boundary of volumes can be smaller than traditionally defined as typical for a rock avalanche, which is often suggested to be close to one million cubic meters (e.g. Evans et al., 2006; Hungr et al., 2014; Pfiffner et al., 2021).

Rock avalanches are important factors driving landscape evolution (Korup et al., 2010; Hewitt et al., 2011). But in addition to shaping landscapes, rock avalanches represent a serious threat to population and infrastructure, both because of the direct impact of the rock mass but also due to their secondary effects (Figure 1; Hermanns et al., 2022), such as dam formation and failure (Costa and Schuster, 1988; Evans et al., 2011; Hermanns et al., 2011), displacement waves (Jørstad, 1968; Fritz et al., 2001; Hermanns et al., 2014), cloud dusts and airblasts (Heim, 1932; De Blasio et al., 2018; Penna et al., 2020). Rock avalanches can also result in secondary mass flows, when they impact on glaciers and incorporate ice and/or snow or if they impact on liquefiable sediments – extending the area of hazard by a factor of 2 and more (e.g. Huggel et al., 2005; Evans et al., 2009; Mitchell et al., 2020). The impact of the rock mass can also cause soft-sediment deformation in valley fills. Folds and faults below the rock avalanche deposit and at a certain distance from its front have been observed in a georadar survey in Romsdalen (Anda and Blikra, 1998; Elvebakk and Blikra, 1999). Soft-sediment deformation has also been documented in relation to rock avalanches impacting fjords, as was the case in Aysén (Chile), where the 2007 earthquake triggered several large rock avalanches that intensively deformed the fjord infill (Lastras et al., 2013). A recent study also pointed out the post-depositional risk posed to the population of settlements built on rock avalanche deposits, owing to radon release from highly fractured rocks. This is the case of the Kinsarvik rock avalanche deposit in western Norway (Rønning et al., under review).

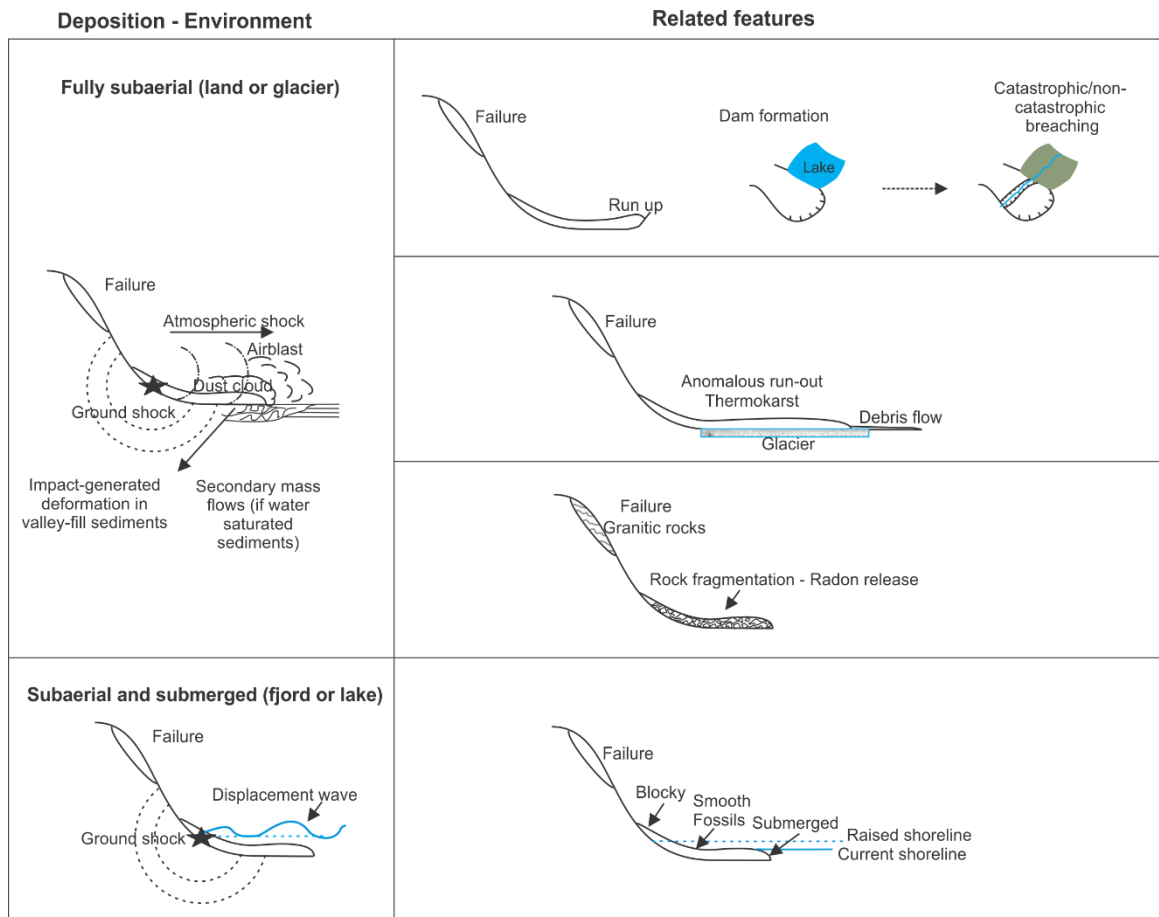


Figure 1. Main primary and secondary effects of rock avalanches by depositional environment observed in Norway.

Up to date, the Geological Survey of Norway has identified 672 large unstable-rock slopes, some of which represent a high risk for society owing to their probability and the potential consequences. Since understanding past events is the key to properly assessing the future scenarios, it is relevant to understand the spatial distribution and main controls of former rock avalanches, as well as their run-outs. Large unstable rock-slopes and the up-to date inventoried rock avalanches deposits in Norway are mainly clustered in the West and in the North (Blikra and Anda, 1997; Blikra et al., 1999; Blikra et al., 2001; Blikra et al., 2002; Blikra et al., 2006; Hermanns et al., 2013; Hermanns et al., 2016; Penna et al., 2022). But while large unstable rock-slopes were mapped systematically, the identification of rock avalanches at country scale has not yet been completed. When looking at the temporal distribution of the rock avalanches deposits, clusters can be observed after glacial retreat and during the Holocene thermal maximum (e.g. Blikra et al., 2002; Schleier et al., 2015; Böhme et al., 2015; Schleier et al., 2017; Hermanns et al., 2017; Hilger et al., 2018; McCurry, 2021; Vick et al., 2022). In 2021, the Geological Survey of Norway by mandate of the Norwegian Energy Resources and Water Directorate, set up a project aiming to analyze the development of unstable rock-slopes, from their initiation to their failure. The project aims to better understand the processes governing the rock-slope deformation over time, the probability of collapses, and the run-out,

among other things. This report focuses on the spatial distribution of the up-to-date mapped rock avalanches, their main features, and some aspects related to their dynamics.

2. METHODOLOGY

2.1 Mapping of rock avalanches

The inventory of rock avalanche deposits was carried out through 1) review of available papers and reports, and interpretation of high-resolution DEMs (freely available on hoydedata.no) and aerial photographs (freely available at norgebilder.no) for deposits located on land, and 2) interpretation of (i) high-resolution bathymetry data, freely available for some places, such as Eikedalsvatnet, Salvatnet or Søre Sunnmøre (hoydedata.no and dybdata.no), (ii) “classified” bathymetry in some fjords, and (iii) our own bathymetric surveys (e.g. Tinnsjø and Vangsmjøse), for deposits located in fjords or lakes. The inventoried rock avalanches were divided in two groups, with the Arctic Circle as a limit in between a northern and a southern group. For the southern group all deposits lie within what is called “Western Norway”.

The rock type in the source area was extracted from the 1:250 000 harmonized bedrock map database (http://geo.ngu.no/kart/berggrunn_mobil/). In case two or more rock types were present in a source area, we assigned the one covering the largest part of the source.

2.2 Significant relief

In this report, we term the potentially erodible relief above a daylighting fictive plane “significant relief”. Its computation was based on the cell-by-cell propagation of an inverted cone with a user-defined inclination from the foot of all slopes (Figure 2). The relief above that daylighting plane corresponds to the potentially erodible relief. Its volume is computed as the sum of the height difference between the plane and the current topography, multiplied by the area of a pixel.

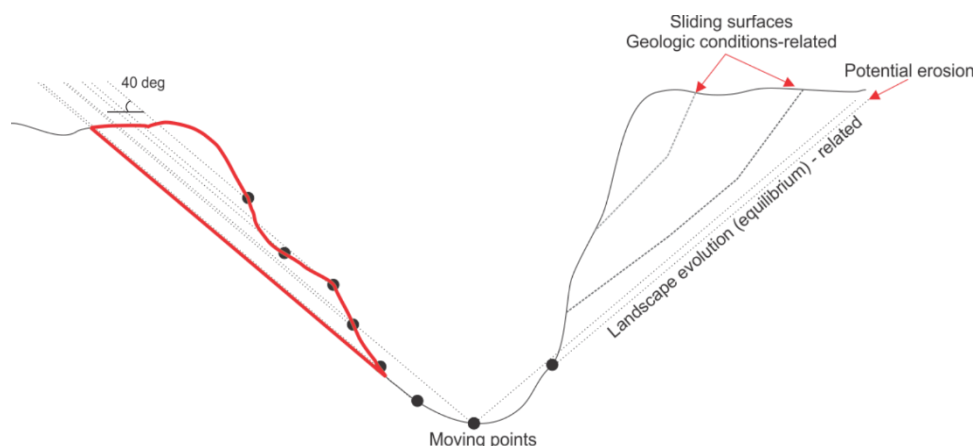


Figure 2. Conceptual diagram of the computation of significant relief. The area delimited in red corresponds to the potentially erodible relief or “significant relief”.

2.3 Longitudinal profiles and cumulative curves

Longitudinal profiles and cumulative curves were created to visualize the relief conditions and the occurrence of rock avalanches on a south to north profile following the orientation of the country (Figure 3). The points with the location of the rock avalanches were projected on the closest location of the profile following the iterative procedure proposed by Hergarten et al. (2014). Rock avalanches are represented as points or increments of a cumulative curve, whereas the topographic conditions are represented by a line showing the mean value, an area bounded by the standard deviation and an area bounded by the minimum and maximum values. The cumulative curve of significant relief is represented by a line showing the increments in the amount of erodible material.

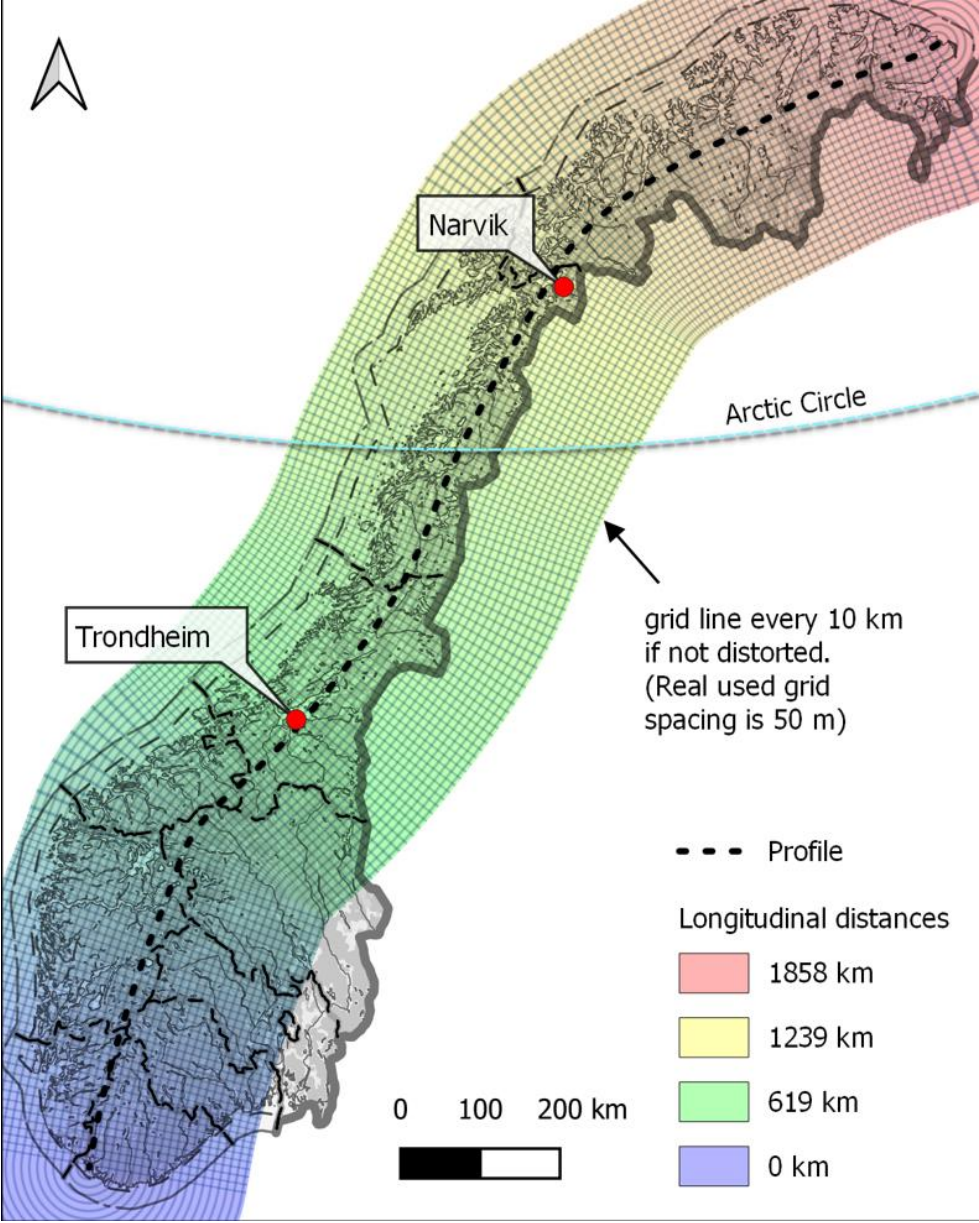


Figure 3. Methodology for the construction of the longitudinal profiles and the cumulative curves.

2.4 Computation of orientation and slope aspect of source areas

The orientation of the source area of each rock avalanche has been calculated using the 10m DTM of Norway (source: Kartverket) and the perimeters of the source areas. For each source area, the normal vector in each cell of the DTM inside the source area's polygon was calculated using the aspect (geodesic method) and slope functions in ArcMap as inputs. Then, a weighted sum of all the normal vectors inside the polygon has been computed. The inverse of the cosine of the slope was used to weight the sum since sloping cells of a DTM represent a larger surface area. Finally, the aspect and slope of the surface represented by the resulting normal vector (i.e., the sum of all the normal vectors) was computed.

Once the orientation of each source area was known, their distribution was analyzed in a rose plot and by calculating a global average orientation of all sliding surfaces. This latter was calculated by summing the horizontal unit vectors derived from the aspect of each source area. The strength of the resulting vector (or mean resultant length) was defined as its length divided by the number of vectors (Borradaile, 2003). Thus, a value of 1 means that all the vectors have the same orientation, while a value close to 0 reflects the absence of preferential orientation.

Preferential orientation is also studied visually using cumulative frequency curves in order to see if there are for example several preferred orientations. Indeed, the sum vector would be close to 0 if there is, for example, a bimodal distribution with opposite modes.

2.5 Computation of volumes involved in rock avalanches

Both the failed and the deposited volumes were calculated using the SLBL method (Jaboyedoff et al., 2020) implemented in an ArcGIS toolbox (<https://github.com/ngu/pySLBL>), which calculate iteratively a new surface based on the average altitude of the neighboring cells. The calculation is done inside a defined polygon representing either the source area or the deposit area. A tolerance can be added to add a curvature, but in this case, no tolerance was used to avoid overestimating the volumes. For the deposits, the volumes computed do not consider the shape of the depositional area, which is a simplification as valleys are often not flat but concave. Especially in narrow impounded valleys sediments accumulating behind the dam can be various tens of meters thick. In addition, post rock avalanche erosion of the deposit itself was not considered. Both factors lead to resulting in an underestimation of the volume. Regarding the source areas, an inverse SLBL was used to allow reconstructing missing volumes. A tolerance could be used in some cases to create a surface going above the topography of the surroundings but defining the tolerance would need to be done specifically for each case. Using no tolerance is however expected to give a rough estimate of the volume, while the exact delimitation of the source area remains uncertain anyway in many cases.

2.6 Angle of reach and Statistical analysis

The angle of reach (Heim, 1932) is commonly used to assess the mobility of rock avalanches and evaluate potential endangered zones. This angle is computed as the angle formed by the distance between the backscarp of the rock avalanche to the distal part of the deposit (L ; measured along the propagation path), and the fall height (H). Scheidegger (1973) established an empirical relationship between the volume of events and the H/L ratio, which is a first order assessment to predict run outs of unstable rock slopes where the volume of the potentially failing mass is known. For this study, we have computed the volumes of the rock avalanche sources and their deposits and analyzed their relationship to the H/L ratio. We have also analyzed the relationship between the average slope angle of the source area and the run out of the events.

The degree of correlation between different parameters is analyzed here using Kendall's τ . This coefficient determines whether two rankings, x and y , are positively associated, independent, or negatively associated, by comparing data pairs (x_1, y_1) and (x_2, y_2) . If, for example, $x_1 > x_2$ and $y_1 > y_2$, then the pair is concordant. Kendall's τ is calculated using the following formula:

$$\tau = \frac{C - D}{\sqrt{\left(\frac{n(n-1)}{2} - T_x\right)\left(\frac{n(n-1)}{2} - T_y\right)}}$$

where C is the number of concordant pairs, D the number of discordant pairs, n the number of data points, T_x the number of ties on x and T_y the number of ties on y (Agresti, 2010). Kendall's τ takes a value between -1 (perfect monotonically decreasing relation) and 1 (perfect monotonically increasing relation). A value of 0 indicates the absence of relation. Kendall's τ does not give any information on the causality, neither does it give information on the slope or the shape of the relation, meaning that a high degree of association can theoretically correspond to a low slope in case of a linear relation. However, if the slope of the relation is low, a little noise on the data is more likely to give a value of Kendall's τ closer to 0 than if the slope is steep.

1. RESULTS

2.7 Mapping of rock avalanche deposits and their source areas

Up to the date of this report, 247 rock avalanche deposits have been mapped in the Norway (Figure 4). Around 45% of the rock avalanches deposits extend entirely on land and 55% are located at least partially under water bodies. Thirty of the rock avalanches deposited on land have obstructed valleys, forming landslide dams that are currently containing a lake upstream or swamps areas (Figure 5A). Owing to erosion, the total amount of rock avalanches forming landslide dams could have been higher.

Several deposits currently on land exhibit raised shorelines or other morphologies indicating that they were previously submerged (Figure 5D). This means that they were exposed by isostatic

rebound, as observed by Vick et al. (2022) in the Skredkallen rock avalanche in Troms County or by Schleier et al. (2017) in a rock avalanche in Gråfonnfjellet in Møre og Romsdal county.

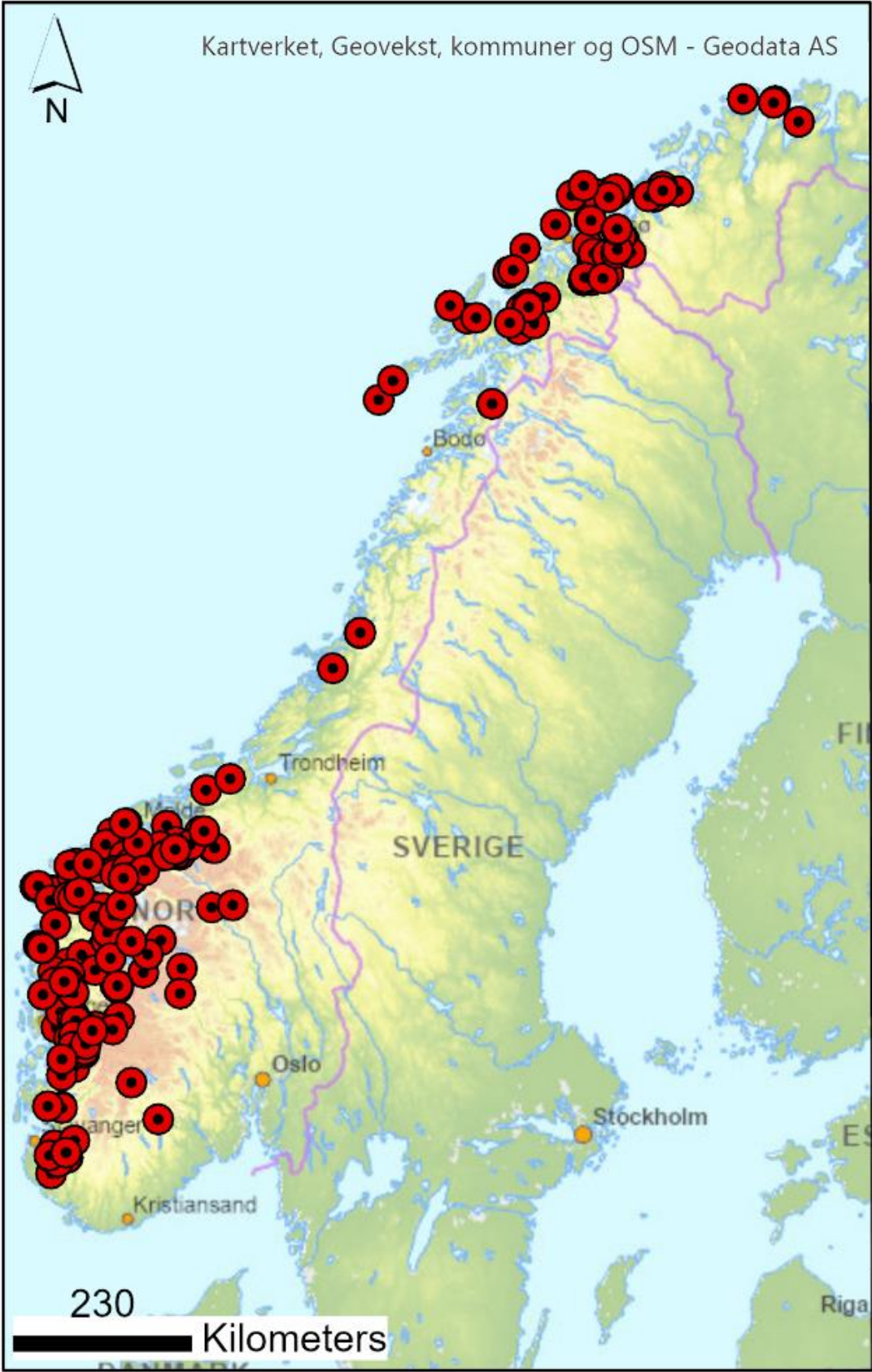


Figure 4. A) Location of the up-to date mapped rock avalanches in Norway. Note: several of these deposits were compiled by Velardi et al. (2020)

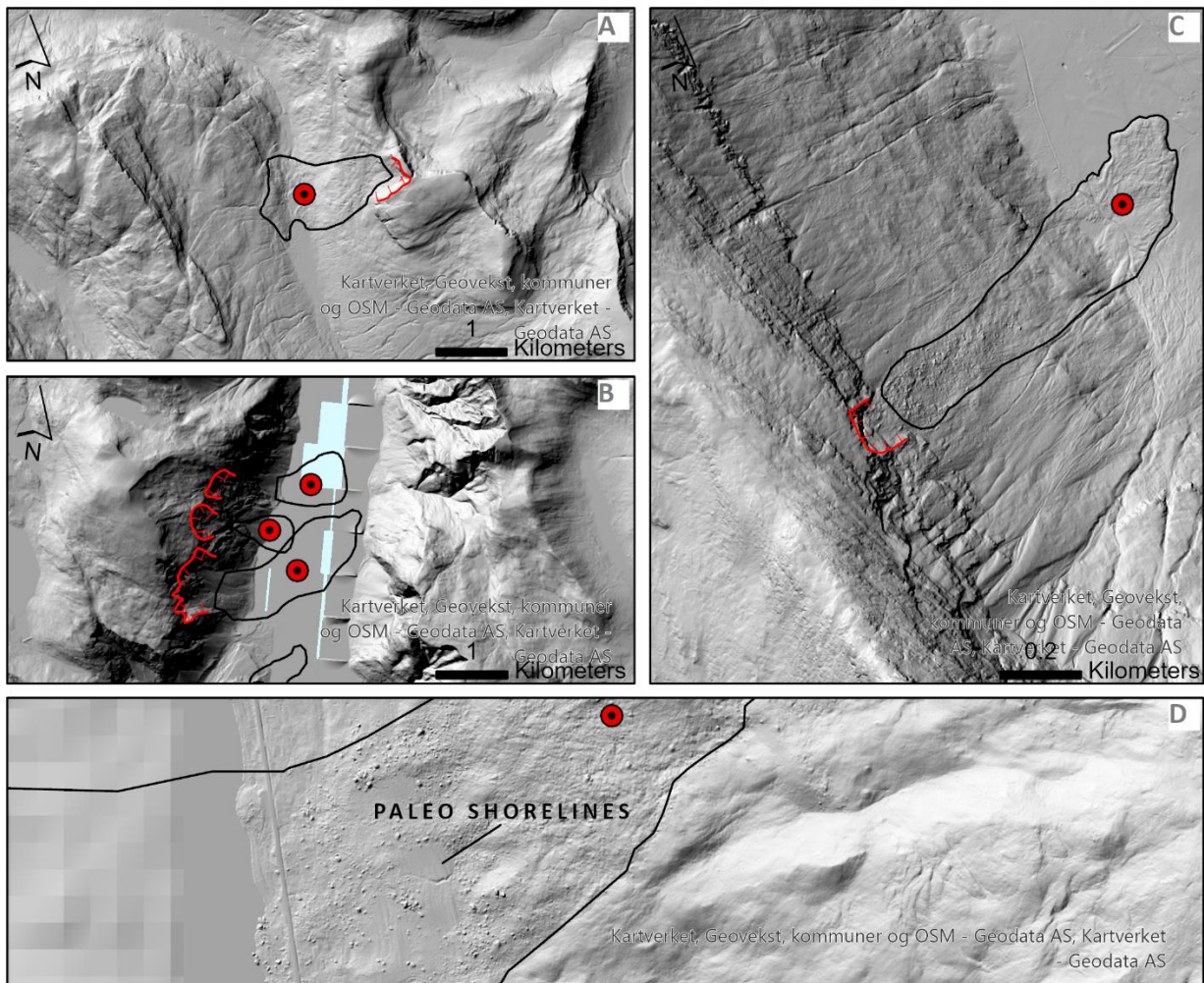


Figure 5. Examples on rock avalanche deposits. A) On land forming a dam and with run-up of the opposite slope. B) Into a water body (Eikedalsvatnet as example). C) On land with unconstrained propagation (26th June 2008 Polvartinden rock-debris avalanche). D) Rock avalanche deposit with subaerial and submerged parts. The presence of raised shorelines could be used as a relative dating method, as they indicate exposure of the rock avalanche deposits due to isostatic rebound.

Most of the mapped rock avalanche deposits are very well preserved, and with no evidence of glacial reworking. Thirteen deposits have potential indicators of permafrost or ice involved at the time of collapse. Eleven of these deposits locate in northern Norway and the main feature suggesting presence of ice at the time of collapse are molards in the distal part of the deposit. One of these deposits (Hølen) seems to have thermokarst in its distal part. The Polvartinden, which occurred in 2008, has documented evidence of presence of permafrost in the source area (Frauenfelder et al., 2018; Figure 5C). In southern Norway, only two collapses have morphologies that indicate potential thermokarst influences, one with detachment at 1500 m a.s.l., on the borders of the Gjegalunds glacier and one with detachment at 1200 m a.s.l. in Eikedals valley.

2.8 Rock avalanche occurrence and significant relief

The rock avalanches are concentrated mainly in the North and in the South of the country, with the highest density in Møre og Romsdal. The altitude of the source areas is variable, ranging from 100 m a.s.l. up to 1940 for a rock avalanche in Rondane (Figure 6A). When comparing the cumulative curve of rock avalanches occurrence, we observe that ca. 70% of them occur in the south of Norway, then the number remains constant up to the north of Narvik when the number of events increases again. The cumulative curve of events presents a very good match with the distribution cumulative curve of available volume of significant relief above 40 degrees (Figure 6B).

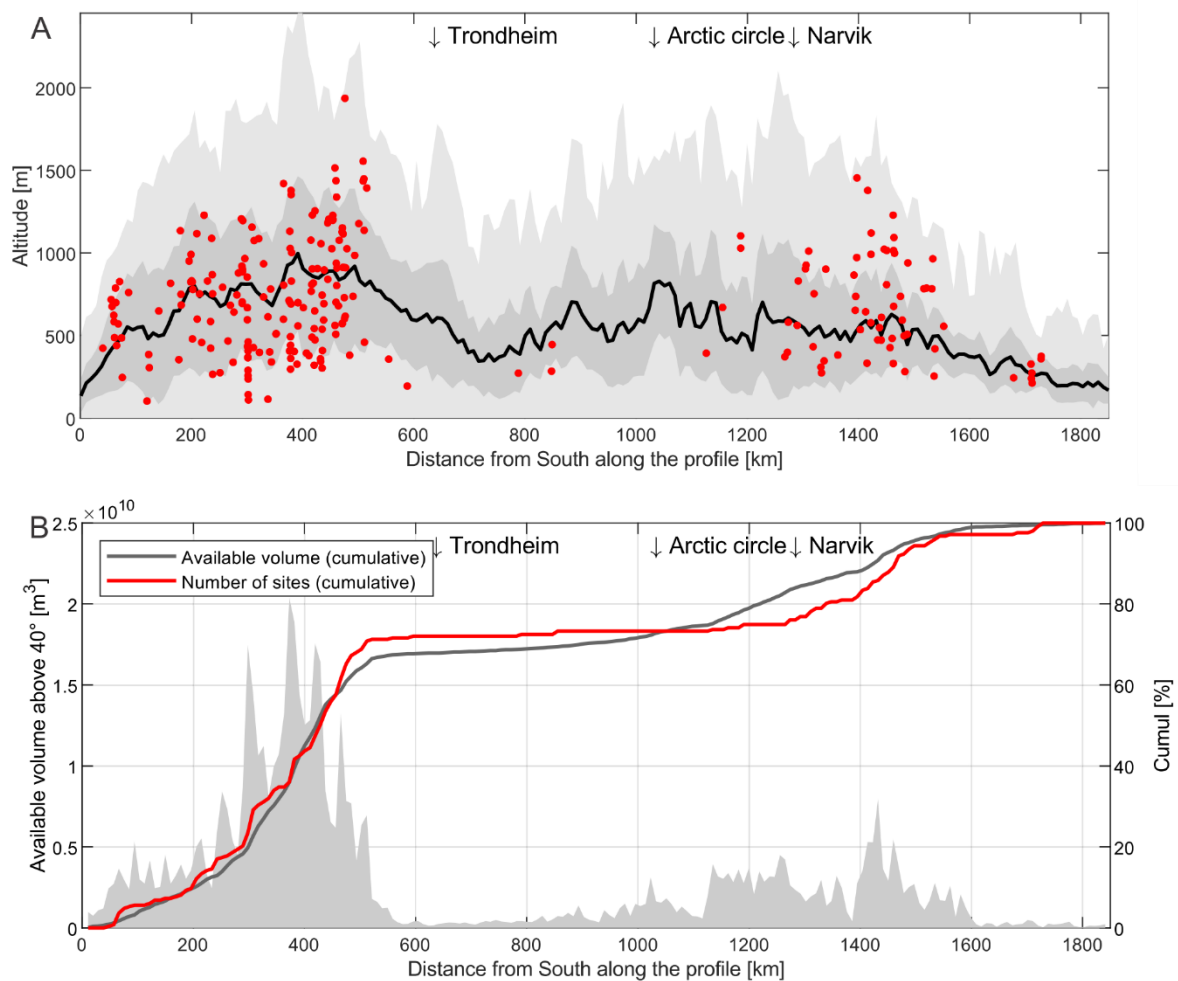


Figure 6. A) Topographic profile (max, min and average altitude) and location of rock avalanches (red dots). B) Profile from south to north showing the available volume of rocks above 40° present in the landscape, and the cumulative curve of rock avalanches and available volume of rocks above 40°.

When looking at the significant relief in the 157 source areas of rock avalanches, we observed that 99% of them are located on significant relief above 30° and where the difference between the current topography and the 30° dipping plane is larger than 30 m. When changing the angle to 35°

the source area of 4 events is not detected (ca. 2.5% of them) and 4% with 40° thickness of 30 m (Figure 7).

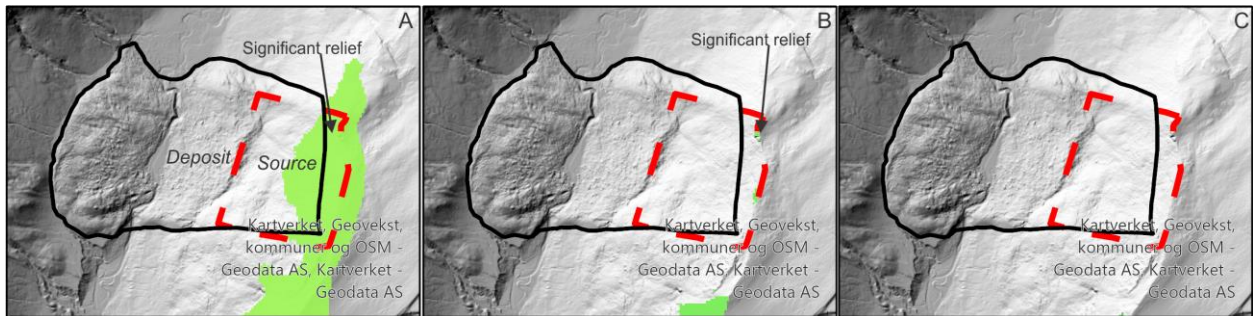


Figure 7. Example of the changes in the extent of the significant relief areas for different angles. A) 30° and thickness over 30m, B) 35° and thickness over 30 m, C) 40° and thickness over 30 m.

2.9 Rock avalanches and lithologies

In the North, the main lithologies involved in rock avalanches are mica-gneisses, mica-schist, metasandstone, amphibolite, followed by gabbro and amphibolite. In the South the dominant unit is the dioritic to granitic gneiss, migmatites, followed by granite and granodiorite.

2.10 Slope aspects and slope of source area

The analysis of azimuth of the source areas does not show a preferential orientation in the South. In the North, they are slightly overrepresented towards the west (between 225° and 315°; Figure 8) and unrepresented towards the south-east (between 90 and 165 degrees). Since the number of rock avalanches is higher in the South, there is almost no preferential orientation for the entire Norway. The mean vector is oriented towards 310, but its strength is only 0.09.

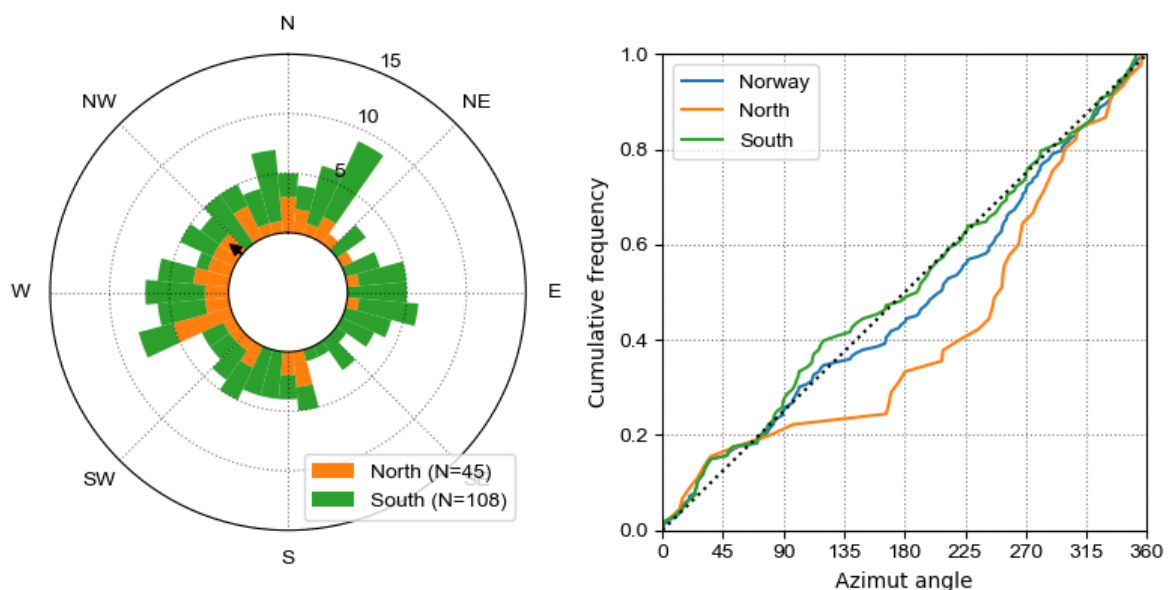


Figure 8. A) Rose diagram with the distribution of slope aspects of the rock avalanches' source area. The black vector indicates the preferred orientation (310), and the vectors' length (0.09) is proportional to its strength. B) Cumulative distribution of the slope aspects of the rock avalanches' source area, showing a preferential orientation in the north, but not in the south, since the latter follows the black dotted line which represents a homogeneous distribution.

When looking at the distribution of slopes in the source area (Figure 9), we observe that the median at country scale is around 45°, but the slopes are steeper in the south than in the north.

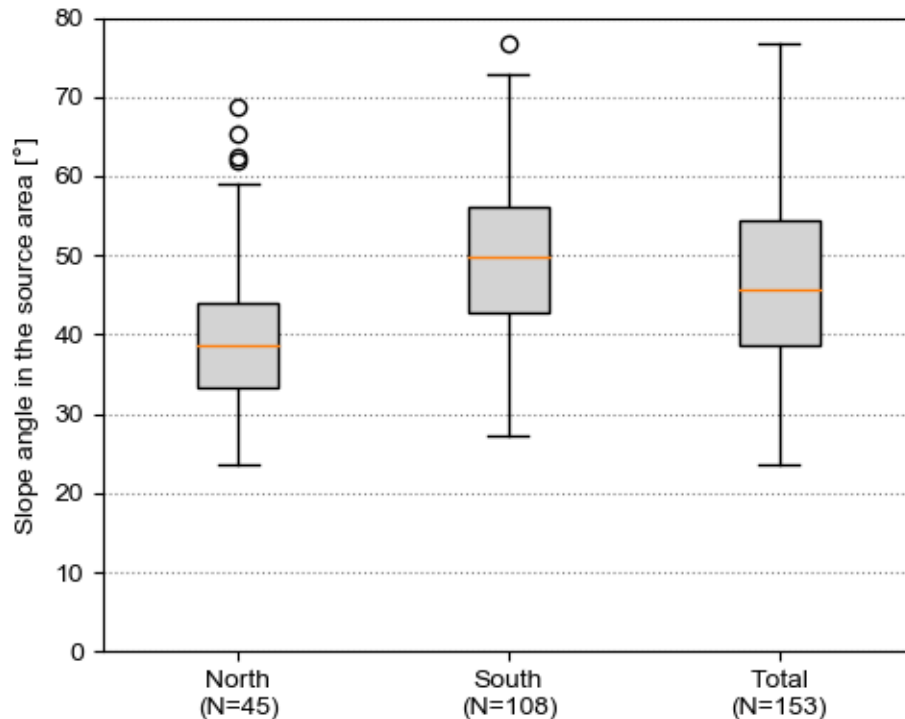


Figure 9. Box plot showing the distribution of slopes at the source areas by region and the entire country. Note: Boxes in boxplot represent 25–75% quartiles and whiskers are 1.5 interquartile ranges from the median. Medians are shown as orange lines.

2.11 Volume estimates

We have computed the volumes of 153 detachment zones and 119 deposits, corresponding in total to 181 rock avalanches. This means that the volume has been estimated for both the source area and the deposit for 91 rock avalanches. The volume could not be calculated for all inventoried rock avalanches because of the preservation degree of the deposits or the detachment zone, or that part of the deposits is below the water. In the North, the volume of the detachment zones ranges from 144 000 m³ to 55.8 *10⁶m³, with a median of 3.66*10⁶m³. In the South, the median volume of detachment zones is slightly smaller at 2.74 *10⁶m³ (Figure 10).

Regarding the volume of the deposits, they range in the North between 143 000 m³ and 45.2 *10⁶m³ (median 1.36*10⁶m³) and in the South from 20 300 m³ to 37.6 *10⁶m³ (median 726 000 m³). It must be pointed out that the volume of some deposits is very low compared to those used to

define rock avalanches (Hermanns et al., 2022). This is because of the methodology used in this study for their computation (see above). By using a tolerance of 0 we are obtaining a minimum volume.

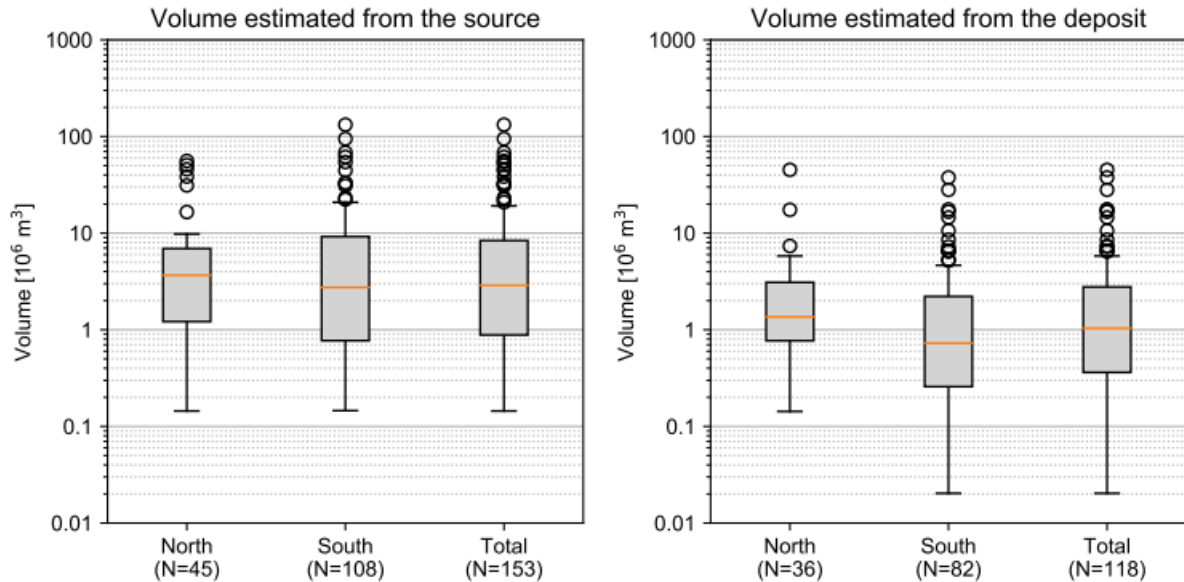


Figure 10. Box plot showing the distribution of detached volumes (source area) and the deposits, by region and the entire country. Note: Boxes in boxplot represent 25–75% quartiles and whiskers are 1.5 interquartile ranges from the median. Medians are shown as orange lines.

As expected, the volume is highly correlated to the surface area of both the source and the deposit (Figure 11). For a similar area, the volume is however larger in the source than in the deposit. This is likely due to a steeper slope at the source area, since a similar area in 2D corresponds to a larger surface when the slope is steeper, but also because of the topographic constrains. Indeed, many of the identified source areas correspond to depressions, where a SLBL with 0 tolerance will create a larger volume than on a relatively flat surface.

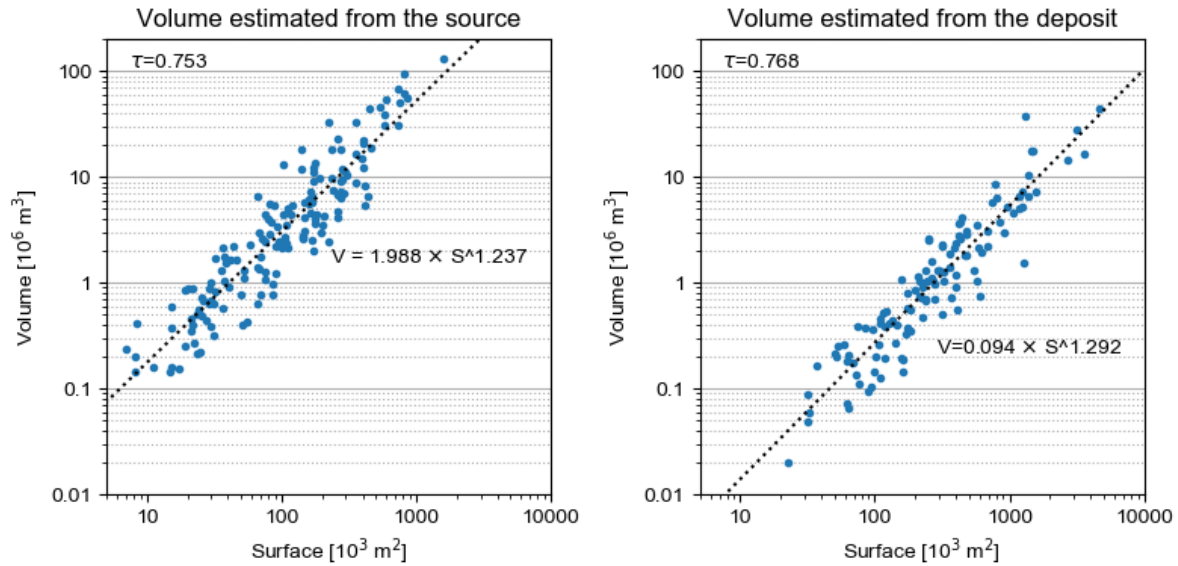


Figure 11. Comparison between the surface and the volume at the source and at the deposit. The volume is logically highly correlated to the area. For an equivalent surface, the SLBL with 0 tolerance gives a larger volume when estimated at the source than when estimated at the deposit. This is likely due to the slope and topographic constraints.

The 91 sites where the volumes are estimated for both the source and the deposit show a good correlation, but the volumes tend to be larger when estimated from the source area compared to the deposit (Figure 12). The differences in volume calculated from the detachment zones and their resultant deposits can be positive or negative and have several causes. 1) The volume computed from deposits can be larger than that computed in source areas because of expansion of the mass due to rock fragmentation and entrainment of material. This is a common feature of rock avalanches described in the literature called “bulking factor” (Hung and Evans, 2004) 2) The volume computed in the source area could be larger than that computed from the deposit because of the higher preservation degree of the source areas. For example, valley bottom deposits may have experienced fluvial erosion or the deposit was inundated by sediments. 3) The tolerance used in the SLBL method (0) can be inappropriate in valley bottom, where a curvature could be necessary to better reproduce the original shape of the valley bottom (see above). 4) The volume computed in the source area can be overestimated if the lower limit is placed too low or, conversely, underestimated if the limit is placed too high. 5) In both cases, the pre-failure topography is unknown, and a relatively high uncertainty is attached to this volume estimation. A site-by-site analysis of the SLBL results would be necessary to lower the uncertainty on the volume estimation.

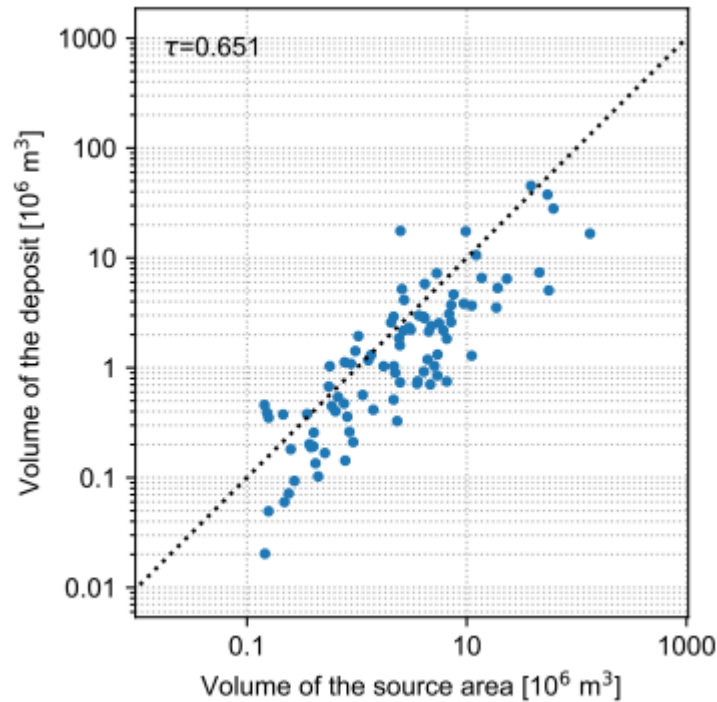


Figure 12. Comparison between the volume measured in the source area vs the volume measured from the resultant deposit. The dashed line is where the source and volume deposits are equivalent.

2.12 Run-out and angles of reach of rock avalanches

Run-out predictions are often based on empirical relationships with rock avalanche volume, or on numerical models (e.g. Scheidegger 1973; Hungr and McDougall, 2009). Environmental and landscape conditions are different in each region, so that the relationships need to be validated and models calibrated with past local events. Here we analyzed the drop height (H) and travel distance (L) of 120 rock avalanches. The maximum measured run-out is ca. 6 km for a rock avalanche with a source area in Dalsfjellet in Troms County. A maximum drop height of ca. 1560 meters was calculated for a rock avalanche that occurred in Romsdalen (Vestland county), followed by a drop height of ca. 1520 meters for a rock avalanche that occurred in Sørfjorden (Vestland county).

We have analyzed the correlation between H/L and volume (V) and of H/L and dip angle of the source area. We observe a correlation between angles of reach and volumes ($\tau = -0.201$ and $\tau = -0.410$; Figure 13). Higher volumes present lower angles of reach. However, the correlation is more significant with the dip of the source area ($\tau = 0.509$; Figure 14) than with the volume. In that case, the correlation is positive, which means that steeper release areas correspond to a larger angle of reach, in other words a shorter run-out.

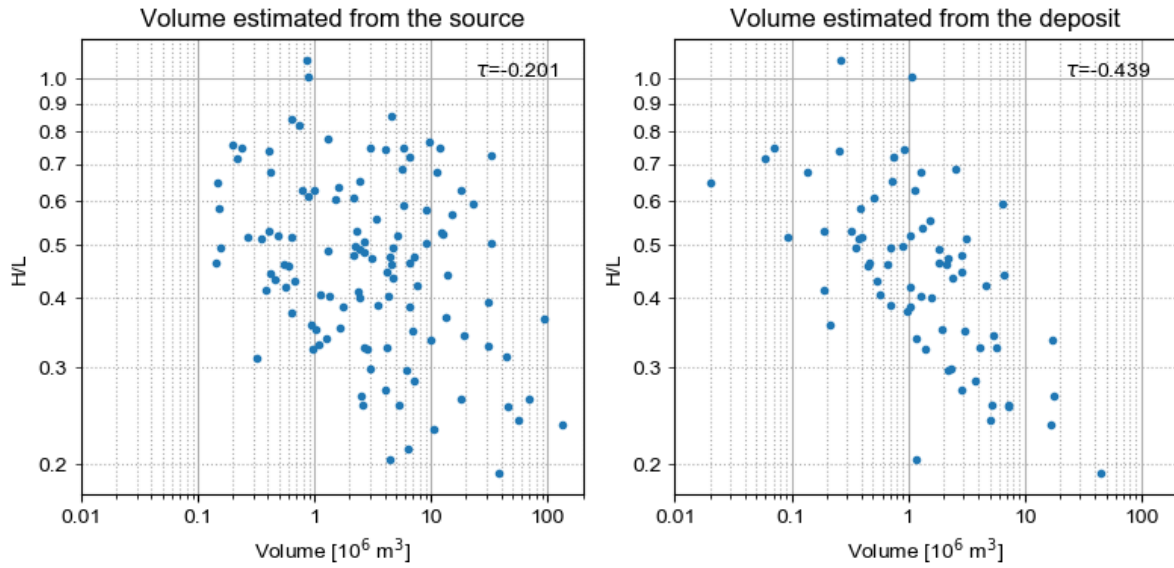


Figure 13. Correlation between H/L and detached volumes.

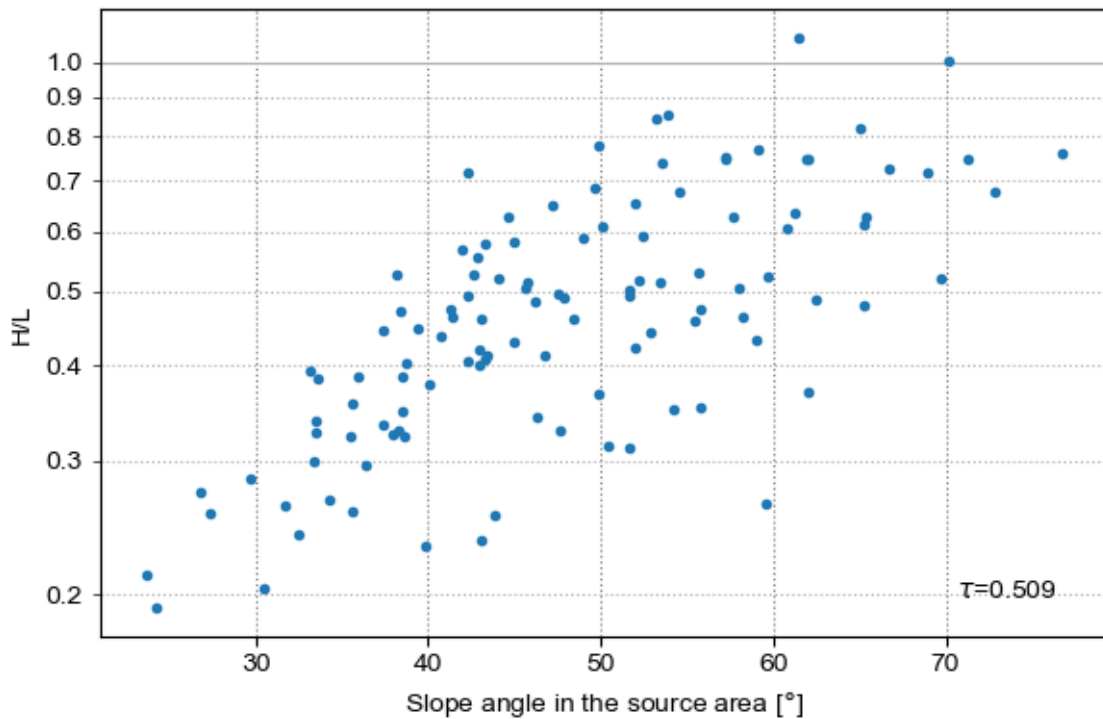


Figure 14. Correlation between H/L and dip angle of the source area.

To date, the relation defined by Scheidegger (1973) is used for the hazard mapping in Norway, with a cut-off value at about 31°. Comparison with the new data presented in this report, however, suggests that this relation may not be appropriate (Figure 15). Nevertheless, a more detailed analysis of the rock avalanche volumes should be undertaken to confirm the new results. A

comparison of travel angles observed in different contexts shows that this may have a strong influence (Figure 16). The few rock avalanches that propagated over a glacier (OG in Figure 16) present a long run-out, while the run-outs are shorter for rock avalanches that propagated unconstrained, both over land and in water bodies.

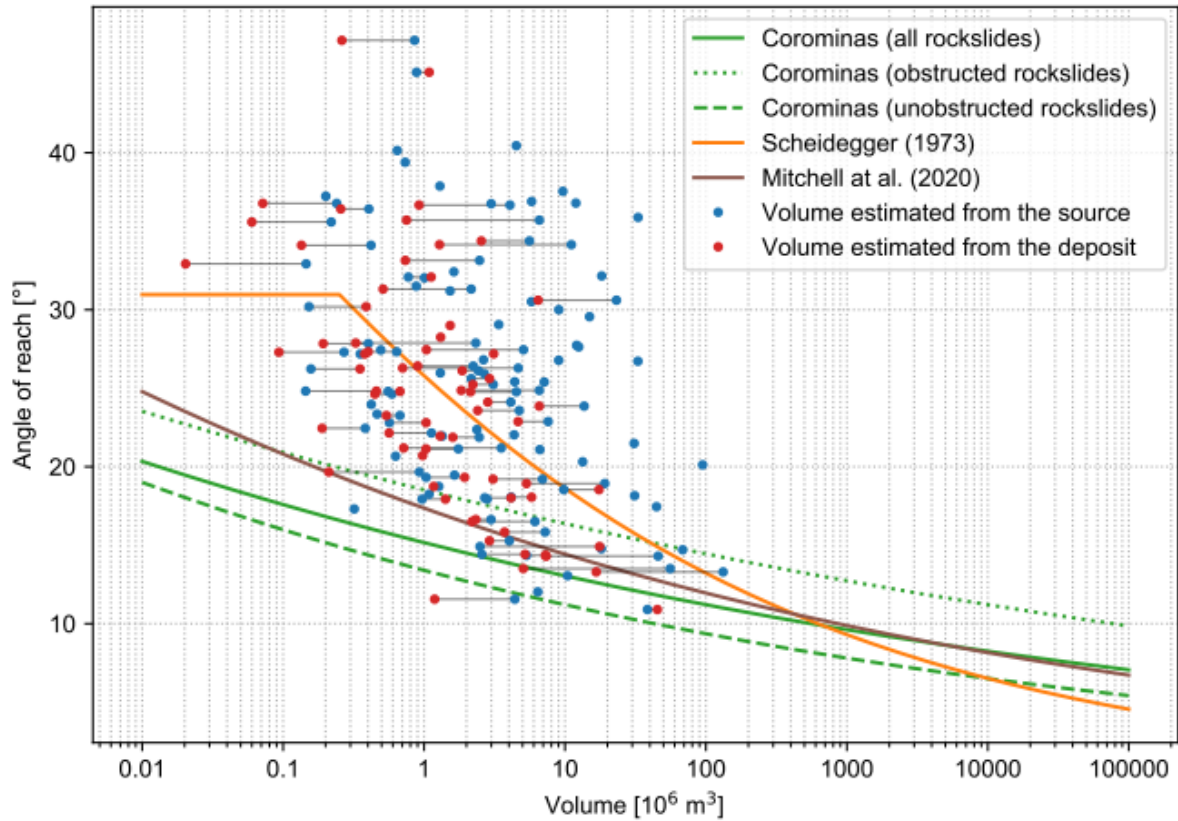


Figure 15. Comparison of the travel angle of the newly mapped events with published relations. The dots connected by a line correspond to the rock avalanches where a volume has been estimated both for the source area and for the deposit.

As we can see in Figure 15, the volumes computed from deposits are typically smaller than those computed in the source area. This is related to the fact that a tolerance of 0 (flat surface) used to reconstruct the lower limit of the deposit does not account for the shape of the depositional surface, such as the curvature of a valley floor, and results in a minimum volume (see above). In the source area, a tolerance of 0 (flat surface) can better reproduce the slope conditions before the collapses. It is generally expected that the volumes of the deposits are larger than those in the source area because of bulking and entrainment of material (e.g. Hungr and Evans, 2004).

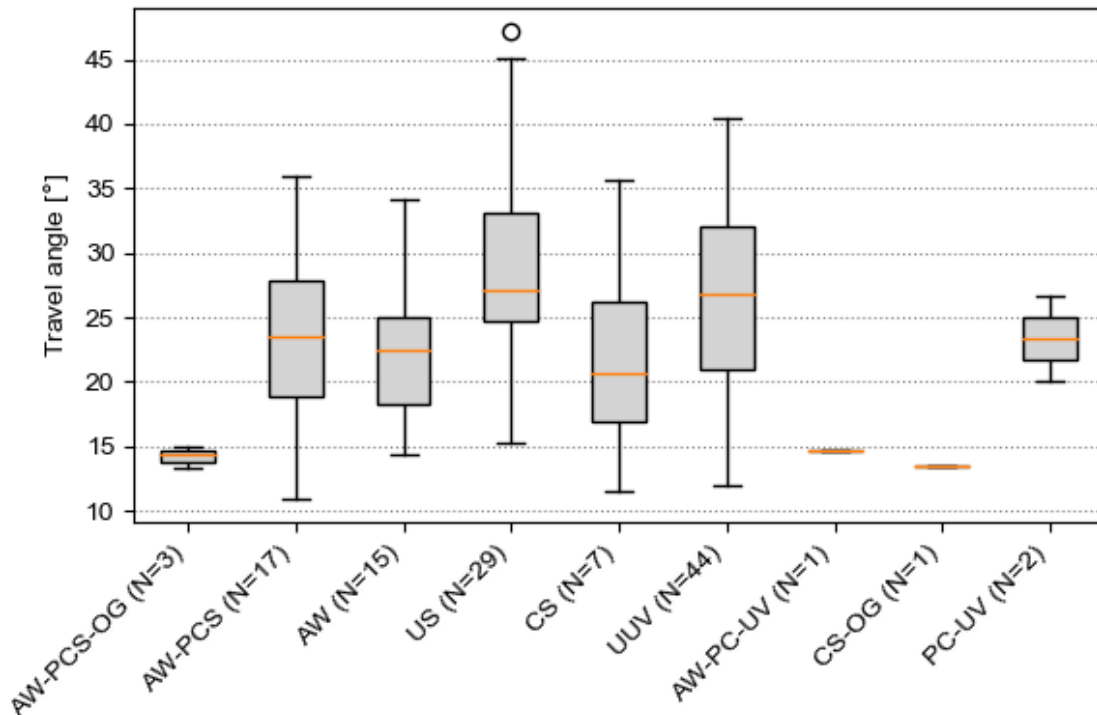


Figure 16. Comparison of travel angles measured in different topographic contexts. AW= against wall, PCS=partially channelized; OG= over glacier. US= unconstrained subaerial, CS= channelized subaerial; UUV=Unconstrained underwater; UV= underwater.

The type of rocks involved in rock avalanches in the North and in the South is not the same. Figure 17 shows that in the North, most rock avalanches developed on mica-gneiss, mica-schist, metasandstone, and amphibolite, while in the South, the largest proportion involved the unit “dioritic to granitic gneiss, migmatites”. The same observation can be made when looking at the rock types associated with mapped large unstable rock-slopes (LURS), both considering all slopes or only those that are moving. However, the proportions are slightly different when comparing rock avalanches and LURS. For example, the proportion of unstable rock slopes involving phyllites is larger than the proportion of rock avalanches involving this lithology, both in the North and in the South.

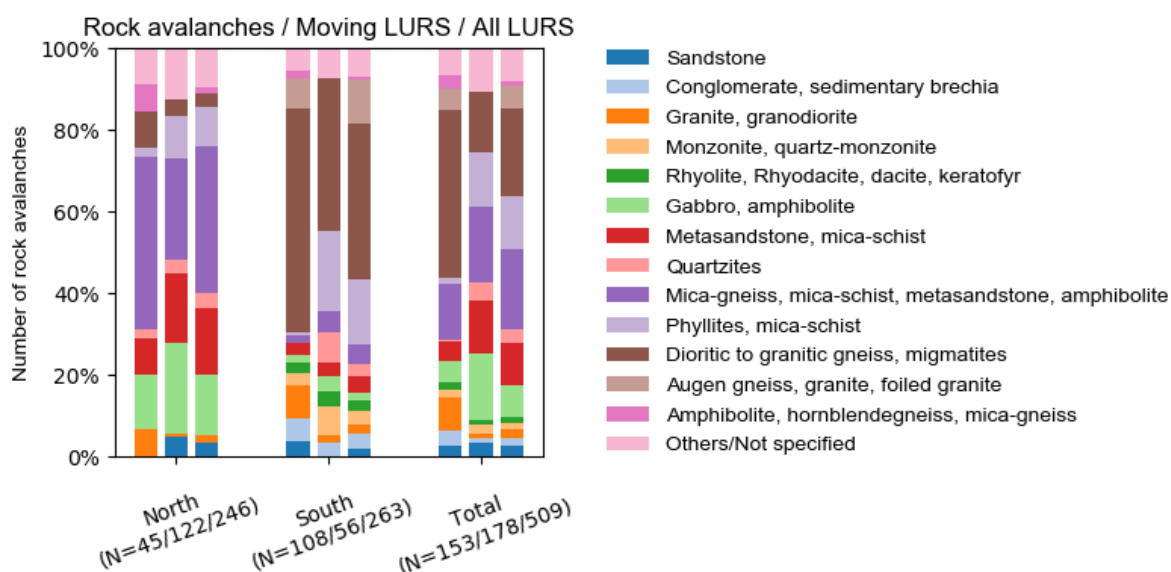


Figure 17. Proportion of rock avalanches, large moving unstable slopes (moving LURS), and large unstable slopes (moving or not) in different lithological contexts. Some lithologies, like “dioritic to granitic gneisses, migmatites” are more represented in the rock avalanches than in the moving LURS, which suggest that they may need less movement prior to failure. Conversely, phyllites and mica-schists are more common in LURS than in rock-avalanches, meaning that they could move without producing a rock avalanche.

3. DISCUSSION AND CONCLUSIONS

In this report we have assessed some of the characteristics of the inventoried rock avalanches in Norway up-to-date. The identified events lay both on land and beneath water bodies in fjords and lakes. Some are very well preserved, while others have been eroded by rivers or buried by fluvial deposits. The deposits with thermokarst features and molards seem to be events that incorporated ice from the source area or the run-out path. Rock avalanches travelling onto ice, entraining ice along their propagation, or permafrost in the detachment zones, have been observed in other parts of the globe such as in the Andes (Fauqué et al., 2009; Hermanns et al., 2015; Schleier et al., 2015) in Alaska (Dufresne et al., 2019) or in Greenland (Morino et al., 2019; Svennevig et al., 2022). Below we discuss the main findings of this study and outline some of its limitations:

3.1 Conditioning factors of rock avalanche occurrence and mobility

The types of rocks involved in rock avalanches in the North and in the South of Norway are different, and this is mostly explained by the different dominant lithologies in both regions. However, the proportion of unstable rock slopes involving phyllites is larger than the proportion of rock avalanches involving this lithology (Figure 17), and this could indicate that unstable rock slopes developed on this type of rocks most likely deform over long periods of time without reaching rapid collapse. The inverse can be observed when looking at the lithological unit “dioritic to granitic gneiss, migmatites”, which is over-represented in rock-avalanches, suggesting that less deformation is

needed prior to collapse. Such relationships, however, should be further explored once the country has been screened systematically and completely.

There is a clear correlation between the relief and the occurrence of rock avalanches, as observed on Figure 6B. In our dataset, significant relief (30 m thickness between the topography and the 30° plane) seems to highlight areas where rock avalanches are more likely to occur.

Earlier analyses, such as Blikra et al. (2001) who analyzed the run-out of 25 rock avalanches mainly from the Western Gneiss Region, show a clear relation between the volume and the angle of reach. Velardi et al. (2020) analyzed around 170 failures and investigated the relation of substrate and morphological aspects in the run-out area. These types of investigations will be carried out using our new dataset once the entire of Norway is mapped. To date, our inventory supports the relationship between volume and angle of reach only to a limited degree. There may be several reasons why our inventory does not follow the same trend:

- Our inventory only covers around 2 orders of magnitude, which is much less, for example, than the inventory of Scheidegger (1973). A trend may be more visible with a greater span of volumes. In any case, the degree of variation for a given volume would still be very large, which means that using such a relation directly would be questionable.
- The volume calculation done for this analysis is very rough. For some rock avalanches there is a relatively large difference between the volume estimated from the source area and the volume estimated from the deposit. However, the volumes are well correlated to the areas of the polygons representing the deposits and volumes estimated from the source and the deposit are well correlated, which implies that the volumes should not be completely wrong, but still depending on the paleo-topographic conditions. Nevertheless, this uncertainty combined with the relatively small magnitude span could be the reason that the correlation is less apparent.
- We did not include uncertainties related to the preservation of rock avalanche events. Including uncertainties related to the preservation degree of events, as used by Velardi et al. (2020) and Kolstad (2021), could allow us to better understand to what extent data quality influences the final relationships.
- Other factors could have a stronger influence on the angle of reach than the rock avalanche volume. One of those factors could, for example, be topography. Figure 14 shows that there is a moderate positive correlation between slope angle in the source area and the angle of reach (i.e., high slope angles lead to shorter run-outs). This could be related to the topography of the propagation area. Indeed, a steep source area is likely to be in a steep valley, where the rock avalanche may lose energy abruptly when it reaches the flatter valley bottom. Figure 16 also shows that different types of propagation area result in different travel angles. A detailed analysis is now needed to explain the observed differences, for example, why unconstrained subaerial rock avalanches present a shorter run-out than the

one colliding with a wall. Further comparison to previous works would help to understand why our observations contrast with previous analyses (Nicoletti and Sorriso-Valvo, 1991; Corominas, 1996; Mitchell et al., 2020; Velardi et al., 2020).

It is likely that multiple parameters, including the volume or type of lithology involved, control the run-out length. Several of the deposits reported here do not necessarily show the same mobility as traditionally attributed to rock avalanches with an angle of reach $<32^\circ$ (e.g. Scheidegger, 1972; Hermanns et al., 2022), and lack of the typical excessive travel length common to rock avalanches (e.g. Hsü, 1975).

A detailed analyses of the mapped rock avalanches will hopefully give some answers and help improve estimates of the likely run-out area of unstable slopes.

3.2 Completeness of the inventory

1) Even if the current inventory includes a significant number of events, and represents the most complete compilation of rock avalanches in Norway up to-date, further work in this project will involve the systematic mapping of rock avalanches at country scale. This will enable us to thoroughly test the robustness of the relationships presented here.

2) The current inventory covers only events that have the size and primary morphologies of rock avalanches (Hermanns et al., 2022). Several events not included in this report have been so far classified as fjellskred/steinskred, and a further assessment of these events is required.

3) This report does not include rock avalanche deposits that have only been identified from sediment cores in fjords or lakes because there is a large uncertainty associated with estimating key diagnostic features (type of event, extent, etc.).

4) In several sites, repeated events on same slopes have been reported (Schleier et al., 2015, Schleier et al., 2017; Hilger et al., 2018). Detailed studies are required to establish other sites with multiple events and the number, extent, and sequence of such events. Considering several overlying deposits to represent one rock avalanche event would lead to false conclusions when assessing the relationship between volume and angle of reach.

5) Periglacial processes (especially in northern Norway) might have reworked rock avalanche deposits, making the identification of some morphological features difficult. Detailed studies are required to differentiate whether such deposits correspond to a spontaneous failure within minutes or rock collapses that take course over several hours (for example, as in Randa, Switzerland; Eberhardt et al., 2004) reworked by periglacial activity. Since the extent of the deposit does not represent that of the primary rock avalanche event, but the result of post-depositional creeping owing to periglacial processes, these events should not be included in analyses of event run-out.

6) Several rock avalanche deposits are strongly eroded making them difficult to reconstruct. For some, the location of the source area is uncertain. Further analysis should include certainty levels to account for these ambiguities.

7) Around 100 unstable rock-slopes have been identified by NGU in Finnmark county. Landscape conditions are suitable for their development and further collapse. The amount of rock avalanche deposits mapped in this county, occurring in coastal cliffs, is expected to rise with interpretation of high-resolution bathymetry.

Because of lack of pre-event topographic conditions and coarse volume estimations, our preliminary data should be taken with caution. However, the compiled data set suggests that multiple events match with volumes earlier reported as rock avalanches (in general $>10^6$ m³ but exceptional down to 10^5 m³) while others might be below this volume range (e.g. Scheidegger, 1973, Hungr, 2006; Mitchell, 2020; Hermanns et al., 2022). Especially the volume range $<10^6$ m³ is strongly underrepresented in most empirical data sets (e.g. Scheidegger, 1973, Hungr, 2006; Mitchell, 2020; Hermanns et al., 2022) and data collected by Corominas (1996) in this range of small volumes relate to a single storm event in the Pyrenees and might thus not be representative. Our data can thus shed light after more careful volume estimations in the discussion of rock avalanche mobility for the lower end of volumes that are considered as rock avalanches so far. Then, these data will represent a good empirical source for hazard zone estimations for rock avalanches at least for the Norwegian setting.

4. REFERENCES

Agresti, A., 2010. Analysis of Ordinal Categorical Data (Second ed.). Wiley Series in Probability and Statistics. New York: John Wiley & Sons. <http://dx.doi.org/10.1002/9780470594001>

Anda, E., and Blikra L.H. 1998. Rock-avalanche hazard in Møre & Romsdal, western Norway. NGI Report 203, 53–57.

Blikra, L.H, Braathen, A., and Skurtveit, E., 2001. Hazard evaluation of rock avalanches; the Baraldsnes – Øteroya Area. Norwegian Geolocial Surey, report 2001.108.

Blikra, L.H., and Anda, E., 1997. Large rock avalanches in Møre og Romsdal, western Norway. NGU Bulletin 433, p. 44-45.

Blikra, L.H., Anda, E., and Longva, O., 1999. Skredfarekartlegging in Lærdal I samband med den nye stamveien Oslo-Bergen. NGU report nr. 96.055.

Blikra, L.H., Braathen, A., Anda, E., Stalsberg, K., and Longva, O., 2002. Rock avalanches, gravitational bedrock fractures and neotectonic faults onshore northern West Norway: Examples, regional distribution and triggering mechanisms. Geological Survey of Norway, report. 2002.016.

Blikra, L.H., Longva, O., Braathen, A., Anda, E., Dehls, J. and Stalsberg, K., 2006. Rock slope failures in Norwegian fjord areas: examples, spatial distribution and temporal pattern. *Landslides from massive rock slope failure*. Springer.

Böhme, M., Oppikofer, T., Longva, O., Jaboyedoff, M., Hermanns, R.L., and Derron, M.-H., 2015. Analyses of past and present rock slope instabilities in a fjord valley: implications for hazard estimations. *Geomorphology* v. 248:, p. 64–474.

Borradaile, G., 2003. *Statistics of Earth Science Data*. Springer-Verlag. ISBN 978-3-662-05223-5

Corominas, J., 1996. The angle of reach as a mobility index for small and large landslides: *Can.Geotech.J.*, v. 33, no. Journal Article, p. 260-271.

Costa, J.E., and Schuster, R.L., 1988. The formation and failure of natural dams. *Geological Society of America Bulletin*, v. 100, n. 7, p. 1054-1068.

De Blasio, F.V., Dattola, G., and Crosta, G.B., 2018. Extremely energetic rockfalls: *Journal of Geophysical Research. Earth Surface*, v. 123, p. 2392-2421.

Eberhardt, E., Stead, D., and Coggan, J.S., 2004. Numerical analysis of initiation and progressive failure in natural rock slopes-the 1991 Randa rockslide. *International Journal of Rock Mechanics & Mining Sciences*, v. 41, p. 69-87.

Elvebakk, H. og Blikra L. H. 1999: Georadarundersøkelser i forbindelse med undersøkelser av fjellskred i Romsdalen, Møre og Romsdal. NGU- rapport 1999.025.

Evans, S. G., Bishop, N. F., Smoll, L. F., Murillo, P. V., Delaney, K. B., and Oliver-Smith, A., 2009. A re-examination of the mechanism and human impact of catastrophic mass flows originating on Nevado Huascarán, Cordillera Blanca, Peru in 1962 and 1970: *Engineering Geology*, v. 108, no. 1-2, p. 96.

Evans, S., Mugnozza, G. S., Strom, A., Hermanns, R., Ischuk, A., and Vinnichenko, S., 2006. Landslides from massive rock slope failure and associated phenomena, *Landslides from Massive Rock Slope Failure*, Springer, p. 03-52.

Evans, S.G., Delaney, K.B., Hermanns, R.L., Strom, A., and Scarascia-Mugnozza, G., 2011. The formation and behaviour of natural and artificial rockslide dams; implications for engineering performance and hazard management, in: *Natural and Artificial Rockslide Dams*, edited by: Evans, S. G., Hermanns, R. L., Strom, A., and Scarascia-Mugnozza, G., Springer, Berlin, Heidelberg, Germany, 1–75.

Fauqué, L., Hermanns, R. L., Hewitt, K., Rosas, M., Wilson, C., Baumann, V., Lagorio, S., and Di Tomasso, I., 2009, Mega-deslizamientos de la pared sur del Cerro Aconcagua y su relación con depósitos asignados a la glaciación pleistocena. *Revista de la Asociación Geológica Argentina*, v. 65, no. 4, p. 691-712.

- Frauenfelder, R., Isaksen, K., Lato, M.J., and Noetzli, J., 2018. Ground thermal and geomechanical conditions in a permafrost-affected high-latitude rock avalanche site (Polvartinden, northern Norway). *The Cryosphere*, v. 12, p. 1531-1550.
- Fritz, H.M., Hager, W.H., Minor, H-E., 2001. Lituya Bay case: rockslide impact and wave run-up. *Sci Tsunami Haz*, v. 19, n. 1, p. 3-22.
- Heim, A., 1932. *Bergsturz und Menschenleben: Vierteljahrsschrift der Naturforschenden Gesellschaft in Zürich*, v. 77, no. Beiblatt Nr. 20, p. 1-214.
- Hergarten, S., Robl, J., and Stüwe, K., 2014. Extracting topographic swath profiles across curved geomorphic features. *Earth Surface Dynamics*, V. 2, p. 97–104.
- Hermanns, R.L., Dahle, H., Bjerke, P.L., Crosta, G.B., Anda, E., Blikra, L.H., Saintot, A., Longva, O. and Eiken, T., 2013. Rockslide dams in Møre og Romsdal county, Norway: examples for the hazard and potential of rockslide dams. In Margottini, C., Canuti, P., and Sassa, K., (eds.). *Landslide science and practice*. Springer, Berlin.
- Hermanns, R. L., Fauqué, L., and Wilson, C. G., 2015. ³⁶Cl terrestrial cosmogenic nuclide dating suggests Late Pleistocene to Early Holocene mass movements on the south face of Aconcagua mountain and in the Las Cuevas–Horcones valleys, Central Andes, Argentina: *Geological Society, London, Special Publications*, v. 399, no. 1, p. 345-368.
- Hermanns, R. L., Oppikofer, T., Roberts, N. J., and Sandøy, G., 2014. Catalogue of historical displacement waves and landslide-triggered tsunamis in Norway. In *Engineering geology for society and territory (Vol. 4, pp. 63–66)*. Cham, Switzerland: Springer.
- Hermanns, R. L., Penna, I. M., Oppikofer, T., Noël, F., and Velardi, G., 2022. Rock Avalanche, in Shroder, J. F., ed., *Treatise on Geomorphology (Second Edition)*: Oxford, Academic Press, p. 85-105.
- Hermanns, R. L., Schleier, M., Böhme, M., Blikra, L. H., Gosse, J., Ivy-Ochs, S., and Hilger, P., 2017. Rock-Avalanche Activity in W and S Norway Peaks After the Retreat of the Scandinavian Ice Sheet, in *Proceedings Workshop on World Landslide Forum 2017*, Springer, p. 331-338.
- Hermanns, R., Oppikofer, T., Böhme, M., Dehls, J., Yugsi Molina, F., and Penna, I., 2016. Rock slope instabilities in Norway: First systematic hazard and risk classification of 22 unstable rock slopes from northern, western and southern Norway, in *Proceedings Proceedings landslides and engineered slopes. Experience, theory and practice: proceedings of the 12th international symposium on landslides*, Napoli, Italy 2016, p. 12-19.
- Hermanns, R.L., Hewitt, K., Strom, A., Evans, S.G., Dunning, S.A., and Scarascia-Mugnozza, G., 2011. The classification of rockslide dams. In Evans, S.G., Hermanns, R.L., Strom, A., and

Scarascia-mugnozza, G. (eds.). Natural and Artificial Rockslide Dams. Lecture Notes in Earth and Sciences, v. 133, p. 581-593. Springer, Berlin.

Hermanns, R.L., Oppikofer, T., Roberts, N.J., and Sandøy, G., 2014. Catalogue of historical displacement waves and landslide-triggered tsunamis in Norway. In Lollino et al. (eds). Engineering Geology for Society and Territory, V. 4, p. 63-66.

Hewitt K., Gosse J. and Clague J.J., 2011. Rock avalanches and the pace of late Quaternary development of river valleys in the Karakoram Himalaya. Geological Society of America Bulletin, 123 (9/10): 1836-1850.

Hilger, P., Hermanns, R. L., Gosse, J. C., Jacobs, B., Etzelmüller, B., and Krautblatter, M., 2018. Multiple rock-slope failures from Mannen in Romsdal Valley, western Norway, revealed from Quaternary geological mapping and ¹⁰Be exposure dating. The Holocene, v. 2 (12), 1841-1854.

Huggel, C., Zraggen-Oswald, S., Haeberli, W., Kaeab, A., Polkvoj, A., Galushkin, I., and Evans, S. G., 2005. The 2002 rock/ice avalanche at Kolka/Karmadon, Russian Caucasus; assessment of extraordinary avalanche formation and mobility, and application of QuickBird satellite imagery, in Evans, S. G., ed., Volume 5: Federal Republic of Germany, Copernicus GmbH on behalf of the European Geophysical Society : Katlenburg-Lindau, Federal Republic of Germany, p. 173-187.

Hungr, O., and Evans, S.G., 2004. Entrainment of debris in rock avalanches: an analysis of a long run-out mechanism. Geological Society of America Bulletin, 116, p. 1240-1252.

Hungr, O., 2006, Rock avalanche occurrence, process and modelling, Volume 49: Netherlands, Springer : Dordrecht, Netherlands, p. 266-243.

Hungr, O., and McDougall, S., 2009. Two numerical models for landslide dynamics analysis. Computers and Geosciences, v. 35 (5), p. 978-992

Hungr, O., Leroueil, S., and Picarelli, L., 2014. The Varnes classification of landslide types, an update: Landslides, v. 11, no. 2, p. 167-194.

Hsü, K. J., 1975, Catastrophic Debris Streams (Sturzstroms) Generated by Rockfalls: Geological Society of America Bulletin, v. 86, no. Journal Article, p. 129-140.

Jaboyedoff, M. Carrea, D. Derron, M.-H. Oppikofer, T. Penna, I. M., Rudaz, B., 2020. A review of methods used to estimate initial landslide failure surface depths and volumes. Eng. Geol. 267, 105478. <https://doi.org/10.1016/j.enggeo.2020.105478>

Jørstad, F.A., 1968. Waves generated by landslides in Norwegian fjordsand lakes. Norwegian Geotechnical Institute, Oslo, 32p.

Kolstad, S. T., 2021. The controlling factors for runout lengths for “steinskred” in Hordaland, developing of a new α - β method for “steinskred” and analyses of the flow behavior “steinskred” event in Modalen, 1953: NTNU.

Korup, O., Densmore, A.L., and Schlunegger, F., 2010. The role of landslides in mountain range evolution. *Geomorphology*, v. 120, n. 1–2, p. 77–9.

Lastras, G., Amblas, D., Calafat, A.M., Canals, M., Frigola, J., Hermanns, R.L., Lafuerza, S., Longva, O., Micallef, A., Sepúlveda, S.A. and Vargas, G., 2013. Landslides cause tsunami waves: insights from Aysén fjord, Chile. *Eos, Transactions American Geophysical Union*, v. 94(34), p.297–298.

McCurry, A., 2021. Paraglacial Rock-Slope Failure Following Deglaciation in Western Norway. In: Beylich, A.A. (eds) *Landscapes and Landforms of Norway*. World Geomorphological Landscapes. Springer, Cham. https://doi.org/10.1007/978-3-030-52563-7_5

Mitchell, A., McDougall, S., Aaron, J., and Brideau, M.-A., 2020. Rock avalanche-generated sediment mass flows: definitions and hazard: *Frontiers in Earth Science*, v. 8, p. 543937.

Mitchell, A., McDougall, S., Nolde, N., Brideau, M.A., Whittall, J., and Aaron, J.B., 2020. Rock avalanche runout prediction using stochastic analysis of a regional dataset. *Landslides*, v. 17, p. 777–792.

Morino, C., Conway, S.J., Sæmundsson, Þ., Helgason, J.K., Hillier, J., Butcher, F.E.G., Balme, M.R., Jordan, C., and Argles, T., 2019. Molards as an indicator of permafrost degradation and landslide processes. *Earth and Planetary Science Letters*, v. 516, p. 136-147.

Nicoletti, P.G., and Sorriso-Valvo, M., 1991. Geomorphic controls of the shape and mobility of rock avalanches: *Geological Society of America Bulletin*, v. 103, no. 10, p. 1365-1373.

NVE rapport 14/2011. Plan for skredfarekartlegging, 86p.

Penna, I.M. Magnin, F. Nicolet, P. Etzelmüller, B., Hermanns, R.L. Böhme, M., Kristensen, L. Nöel, F. Bredal, M., and Dehls, J.F., 2022. Permafrost controls the displacement rates of large unstable rock-slopes in subarctic environments, *Global and Planetary Change*, 104017, <https://doi.org/10.1016/j.gloplacha.2022.104017>.

Penna, I.M., Hermanns, R.L., Nicolet, P., Morken, O.A., Dehls, J., Gupta, V., and Jaboyedoff, M., 2020. Airblasts caused by large slope collapses: *GSA Bulletin*, v. 133(5-6), p. 939-948.

Pfiffner, O. A., Hermanns, R. L., Davies, T. R., and Clague, J. J., 2021, Editorial: Rock Avalanches: *Frontiers in Earth Science*, v. 9, no. 34.

Rønning, J.S., Böhme, M., Fredin, O., Hansen, L., Hermanns, R.L., Ofstad, F., Penna, I.M., Solli, A., Høst, J., under review. Rock-avalanche deposit causes extreme high indoor radon concentrations in Kinsarvik, Ullensvang Municipality, Western Norway.

Scheidegger, A.E., 1973. On the prediction of the reach and velocity of catastrophic landslides. *Rock Mech. Felsmechanik. Mecanique des Roches*, v. 5, p. 231-236,

Schleier, M., Hermanns, R.L., Gosse, J.C., Oppikofer, T., Rohn, J., and Tønnesen, J.F., 2017. Subaqueous rock-avalanche deposits exposed by post-glacial isostatic rebound, Innfjorddalen, Western Norway. *Geomorphology*, v. 189, p. 117-133.

Schleier, M., Hermanns, R.L., Rohn, J., and Gosse, J.C., 2015. Diagnostic characteristics and paleodynamics of supraglacial rock avalanches, Innerdalen, Western Norway. *Geomorphology*, v. 245, p. 23-39.

Svennevig, K., Hermanns, R. L., Keiding, M., Binder, D., Citterio, M., Dahl-Jensen, T., Mertl, S., Sørensen, E. V., and Voss, P. H., 2022. A large frozen debris avalanche entraining warming permafrost ground—the June 2021 Assapaat landslide, West Greenland. *Landslides*, p. 1-19.

Velardi, G., Hermanns, R. L., Penna, I., and Böhme, M., 2020. Prediction of the Reach of Rock Slope Failures Based on Empirical Data From Norway, ISRM International Symposium - EUROCK 2020: physical event not held, International Society for Rock Mechanics and Rock Engineering, p. 8.

Vick, L.M., Mikkelsen, M., Corner, G.D., Kjellman, S.E., Trønnes, L., Hormes, A., Allaart, L., and Bergh, S.G., 2022. Evolution and temporal constraints of a multiphase postglacial rock slope failure. *Geomorphology*, v. 398. <https://doi.org/10.1016/j.geomorph.2021.108069>



GEOLOGICAL
SURVEY OF
NORWAY

· NGU ·

Geological Survey of Norway
PO Box 6315, Sluppen
N-7491 Trondheim, Norway

Visitor address
Leiv Eirikssons vei 39
7040 Trondheim

Tel (+ 47) 73 90 40 00
E-mail ngu@ngu.no
Web www.ngu.no/en-gb/